East European Journal of Physics. 2. 610–621 (2026)
DOI: 10.26565/2312-4334-2026-2-68 ISSN 2312-4334

AXIALLY SYMMETRIC SHARMA MITTAL HOLOGRAPHIC DARK ENERGY IN THE BRANS-DICKE THEORY

Suresh Kadali, **Neelima Davuluri***
Department of Mathematics and Statistics, GITAM (Deemed to be University), Visakhapatnam-530045, India
*Corresponding Author e-mail: neeludavuluri@gmail.com
Received March 2, 2025; revised May 3, 2025; accepted May 24, 2026

This study investigates Sharma–Mittal Holographic Dark Energy (SMHDE) within the context of Brans–Dicke theory of gravitation in an Axially Symmetric Cosmological Model. By employing Sharma–Mittal entropy, which provides a unifying generalization of Tsallis and Rényi entropies, a modified form of holographic dark energy density is formulated to incorporate non-extensive thermodynamic effects. The corresponding field equations are derived and solved to obtain exact analytical solutions. Furthermore, key cosmological parameters such as the EoS parameter, deceleration parameter, and squared speed of sound are systematically analyzed to examine the dynamical behaviour and stability of the model. The results indicate that the proposed framework successfully describes the late-time accelerated expansion of the cosmos while also accommodating possible anisotropies in the early cosmos. Overall, the model presents a consistent and physically viable extension of conventional holographic dark energy scenarios within scalar–tensor gravitational theory.

Keywords: *Sharma–Mittal Entropy; Holographic Dark Energy; Brans–Dicke Theory; Axially Symmetric Metric*

PACS: 95.36.+x, 98.80.-k, 98.80.jk, 11.10.Kk

1. INTRODUCTION

The theory of cosmology and gravitation is one of the great achievements of modern theoretical physics. The discovery of SNe Ia gave us the first evidence of the accelerated expansion of the Universe [1-2]. This discovery was then corroborated by independent measurements made from the observation of the cosmic microwave background (CMB) radiation and the study of the large scale structure [3-4]. All these observations show that our current Universe is dominated by a negative pressure mysterious constituent named dark energy (DE) and this component is responsible for driving the Universe towards an accelerated expansion. Observations have shown that DE comprises 70-75% of the energy density of the current universe [5-6]. But, still, the origin of DE is not known.

Many DE models have been proposed by many researchers in order to understand the nature of DE. Among those models, one interesting model is the holographic dark energy (HDE) model. The idea of HDE arises from the idea of the holographic principle postulated by 't Hooft and Susskind [7-8], which says that the number of degrees of freedom in any physical system is proportional to its boundary area and not its volume.

The holographic dark energy (HDE) model is motivated by the holographic principle proposed by 't Hooft and Susskind [7–8], which states that the physical degrees of freedom of a system are determined by its boundary area rather than its volume. Based on this idea, Cohen et al. [9] established a relation between the ultraviolet (UV) and infrared (IR) cutoffs by requiring that the vacuum energy contained in a region of size L should not exceed the mass of a black hole of the same size. This condition leads to the holographic dark energy density

$$\rho_{de} = 3k^2 M_p^2 L^{-2}$$

where k is a dimensionless holographic parameter, $M_p = (8\pi G)^{-1/2}$ is the reduced Planck mass, G is Newton's gravitational constant, and L denotes the infrared cutoff length scale. Later, Li [10] proposed the future event horizon as the IR cutoff and obtained a cosmologically viable HDE model capable of describing the observed accelerated expansion of the universe.

The conventional HDE model is constructed using the Bekenstein–Hawking entropy-area relation,

$$S_{BH} = \frac{A}{4G}$$

where A is the horizon area.

Since gravitational systems are characterized by long-range interactions and non-extensive thermodynamic behavior, generalized entropy formalisms have been proposed to extend the standard entropy description. Among these, Tsallis entropy [11] and Rényi entropy [12] have attracted considerable attention in cosmological applications. A more general entropy framework was introduced by Sharma and Mittal [13], which unifies both Tsallis and Rényi entropies through two independent parameters.

Cite as: S. Kadali, N. Davuluri, East Eur. J. Phys. 2, 610 (2026), https://doi.org/10.26565/2312-4334-2026-2-68

The Sharma–Mittal entropy is defined as

$$S_{SM} = \frac{1}{s}[(1 + lS_T)^{\frac{s}{l}} - 1]$$

where S_T denotes the Tsallis entropy, while s and l represent the deformation and non-extensivity parameters, respectively.

To formulate Sharma–Mittal holographic dark energy (SMHDE), the standard Bekenstein–Hawking entropy used in the HDE framework is replaced by Sharma–Mittal entropy. Taking $S_T = S_{BH} = A/4$ (in natural units $G = 1$) and considering the Hubble horizon $L = H^{-1}$, whose area is $A = \frac{4\pi}{H^2}$, the Sharma–Mittal entropy becomes

$$S_{SM} = \frac{1}{s}\left[\left(1 + \frac{\pi l}{H^2}\right)^{\frac{s}{l}} - 1\right]$$

where H is the Hubble parameter.

Using the holographic relation between entropy and dark energy density, Jawad et al. [14] and Iqbal and Jawad [15] obtained the Sharma–Mittal holographic dark energy density as

$$\rho_{de} = \frac{3k^2 S_{SM}}{8\pi L^4} = \frac{3k^2 H^4}{8\pi s}\left[\left(1 + \frac{\pi l}{H^2}\right)^{\frac{s}{l}} - 1\right]$$

where H is the Hubble parameter.

In contrast to conventional HDE, the SMHDE theory takes into account the effects of the entropy due to non-extensive thermodynamics using the parameters s and l. These correction terms have substantial impacts on the dynamics of the universe, which can explain not only inflation but also acceleration at late times in the same theory [16-17]. Besides, some recent studies have demonstrated that SMHDE models can offer stable evolution and phantom crossing in cosmology.

At the same time, scalar-tensor theories of gravity offer a viable alternative explanation of cosmic acceleration. One of the most successful generalizations of general relativity is the Brans-Dicke (BD) theory [18], proposed by Brans and Dicke in 1961. The BD scalar field inherently satisfies Mach's principle and acts as an important ingredient in explaining cosmological processes [19–20]. Some of the authors have studied the possibility of applying HDE and generalized entropy-based dark energy models within the framework of BD gravity, highlighting their peculiarities and stability properties [21-23].

On the other hand, observations of the anisotropies in the cosmic microwave background (CMB) and the formation of large-scale cosmic structures suggest that the early Universe may not have been perfectly isotropic. Therefore, anisotropic cosmological models, such as Bianchi-type models and axially symmetric models, play an important role in understanding the dynamical evolution of the Universe [24-25]. Axially symmetric universes provide a more general geometric framework than the standard Friedmann–Robertson–Walker (FRW) model and help to describe deviations from perfect isotropy in the early stages of cosmic evolution.

These developments motivate the present study, in which we investigate the Sharma–Mittal holographic dark energy model in an axially symmetric framework within the Brans–Dicke theory of gravity. The generalized Sharma–Mittal entropy is incorporated into the holographic energy density, and an anisotropic geometry is considered to examine the combined effects of entropic deformation, scalar–tensor coupling, and directional anisotropy on the evolution of the Universe. The corresponding field equations are derived, and important cosmological parameters, such as the equation of state parameter, the deceleration parameter, and the squared speed of sound, are analyzed to study the dynamical behavior and stability of the model.

The present work aims to provide a deeper understanding of the role of generalized entropy corrections in scalar–tensor theories and their implications for the evolution of the Universe.

2. METRIC AND FIELD EQUATIONS

The Axially Symmetric cosmological model can be defined as

$$ds^2 = dt^2 - A^2\left[dx^2 + f^2 d\Phi^2\right] - B^2 dz^2 \tag{1}$$

where A and B are functions of time t only and f is function of x .
Brans-Dicke field equations are given by

$$R_{ij} - \frac{1}{2}R\, g_{ij} = \frac{-8\pi}{\phi}T_{ij} - \omega\phi^{-2}\left(\phi_{,i}\phi_{,j} - \frac{1}{2}g_{ij}\phi_{,k}\phi^{,k}\right) - \frac{1}{\phi}\left(\phi_{i:j} - g_{ij}\phi_{,k}{}^{,k}\right) \tag{2}$$

and

$$\Box\phi = \frac{8\pi}{3 + 2\omega}T \tag{3}$$

Here ω is constant, $G_{ij} = R_{ij} - \frac{1}{2}R\,g_{ij}$ is the Einstein tensor, R_{ij} is Ricci curvature tensor, R is Ricci scalar and T_{ij} is the matter's energy momentum tensor,ϕ is the Brans-Dicke's scalar field, g_{ij} is the space time's metric tensor.
It's energy conservation equation is

$$T_{:j}^{\ ij} = 0 \tag{4}$$

The equation of the energy momentum tensors for matter and dark energy as follows

$$T_{ij} = T_{ij}^{m} + T_{ij}^{\wedge} \tag{5}$$

where T_{ij}^{m} and $T_{ij}^{\wedge}$ are represents the energy momentum tensor for DM and DE respectively and defined as

$$T_{ij}^{m} = (\rho_{de} + p_{de})\,u_i u_j - p_{de} g_{ij} \qquad \text{and} \qquad T_{ij}^{\Lambda} = \rho_m u_i u_j \tag{6}$$

Then the corresponding energy momentum tensor is given by

$$T_{ij} = diag\ \ (\rho_{de} + \rho_{de}, -p_{de}, -p_{de}, -p_{de}) \tag{7}$$

where ρ_m and ρ_{de} are the energy densities of DM and the DE respectively and p_{de} is the DE's pressure.
The field equations (2) and (3) for the metric in Eq. (1) can now be expressed using Eq. (7).

$$-\frac{8\pi}{\phi}p_{de} = \frac{\ddot{A}}{A} + \frac{\ddot{B}}{B} + \frac{\dot{A}\dot{B}}{AB} + \frac{\omega}{2}\frac{\dot{\phi}^2}{\phi^2} + \frac{\dot{\phi}}{\phi}\left(\frac{\dot{A}}{A} + \frac{\dot{B}}{B}\right) + \frac{\ddot{\phi}}{\phi} \tag{8}$$

$$-\frac{8\pi}{\phi}p_{de} = \frac{\ddot{A}}{A} + \frac{\ddot{B}}{B} + \frac{\dot{A}\dot{B}}{AB} - \frac{f''}{A^2 f} + \frac{\omega}{2}\frac{\dot{\phi}^2}{\phi^2} + \frac{\dot{\phi}}{\phi}\left(\frac{\dot{A}}{A} + \frac{\dot{B}}{B}\right) + \frac{\ddot{\phi}}{\phi} \tag{9}$$

$$-\frac{8\pi}{\phi}p_{de} = 2\frac{\ddot{A}}{A} + \frac{\dot{A}^2}{A^2} - \frac{f''}{A^2 f} + \frac{\omega}{2}\frac{\dot{\phi}^2}{\phi^2} + 2\frac{\dot{A}}{A}\frac{\dot{\phi}}{\phi} + \frac{\ddot{\phi}}{\phi} \tag{10}$$

$$\frac{8\pi}{\phi}(\rho_{de} + p_{de}) = \frac{\dot{A}^2}{A^2} + \frac{2\dot{A}\dot{B}}{AB} - \frac{\omega}{2}\frac{\dot{\phi}^2}{\phi^2} + \left(2\frac{\dot{A}}{A} + \frac{\dot{B}}{B}\right)\frac{\dot{\phi}}{\phi} \tag{11}$$

And the energy conservation equation is

$$\dot{\rho_m} + \dot{\rho_{de}} + (\rho_m + \rho_{de} + P_{de})\left(\frac{2\dot{A}}{A} + \frac{\dot{B}}{B}\right) = 0 \tag{12}$$

In this case, ordinary differentiation w.r.t t is represented by the notation dot $(\cdot)$ and differentiation w.r.t x is represented by notation dash $(')$.
From Eqs. (8)-(11), it is observed that the terms containing $f(x)$ depend only on the spatial coordinate (x), whereas the remaining terms are functions of cosmic time (t). Since both sides are functions of independent variables, they must be equal to a constant. Therefore, we set

$$\frac{f''}{f} = \alpha^2 \tag{13}$$

where α^2 is an arbitrary separation constant.

For the particular case $\alpha = 0$, (13) reduces to $f'' = 0$, whose solution is

$$f(x) = \alpha_1 x + \alpha_2$$

where α_1 and α_2 are constants of integration.

Consequently, the field equations can be rewritten as

$$-\frac{8\pi}{\phi}p_{de} = \frac{\ddot{A}}{A} + \frac{\ddot{B}}{B} + \frac{\dot{A}\dot{B}}{AB} + \frac{\omega}{2}\frac{\dot{\phi}^2}{\phi^2} + \frac{\dot{\phi}}{\phi}\left(\frac{\dot{A}}{A} + \frac{\dot{B}}{B}\right) + \frac{\ddot{\phi}}{\phi} \tag{14}$$

$$-\frac{8\pi}{\phi}p_{de} = \frac{\ddot{A}}{A} + \frac{\ddot{B}}{B} + \frac{\dot{A}\dot{B}}{AB} + \frac{\omega}{2}\frac{\dot{\phi}^2}{\phi^2} + \frac{\dot{\phi}}{\phi}\left(\frac{\dot{A}}{A} + \frac{\dot{B}}{B}\right) + \frac{\ddot{\phi}}{\phi} \tag{15}$$

$$-\frac{8\pi}{\phi}p_{de} = 2\frac{\ddot{A}}{A} + \frac{\dot{A}^2}{A^2} + \frac{\omega}{2}\frac{\dot{\phi}^2}{\phi^2} + 2\frac{\dot{A}}{A}\frac{\dot{\phi}}{\phi} + \frac{\ddot{\phi}}{\phi} \tag{16}$$

$$\frac{8\pi}{\phi}(\rho_{de} + p_{de}) = \frac{\dot{A}^2}{A^2} + \frac{2\dot{A}\dot{B}}{AB} - \frac{\omega}{2}\frac{\dot{\phi}^2}{\phi^2} + \left(2\frac{\dot{A}}{A} + \frac{\dot{B}}{B}\right)\frac{\dot{\phi}}{\phi} \tag{17}$$

3. SOLUTIONS OF THE FIELD EQUATIONS

Equations (14)-(17) form a system of four different equations with seven unknown variables; $\rho_m, \rho_{de}, p_{de}, \omega_{de}, A, B$ and ϕ. Hence to solve the system of equations we assume
(i)Firstly the relationship between the metric potentials A and B as

$$B = A^{k_1} \tag{18}$$

Here k_1 is a constant.
Following the works of R. C. Johri and R. Sudharsan [26], R. C. Johri and K. Desikan [27], and Diksha Trivedi [28],
(ii)Secondly, we assume a power-law relationship between the Brans–Dicke scalar field ϕ and the average scale factor $a(t)$, given by

$$\phi \propto [a(t)]^{k_2},$$

where k_2 is a constant power-law index.

Such a relation has been extensively employed in the literature to investigate various cosmological aspects of scalar–tensor theories. Motivated by its physical significance and to simplify the highly nonlinear field equations, we adopt the following form:

$$\phi = \phi_0 [a(t)]^{k_2} \tag{19}$$

where ϕ_0 and k_2 are arbitrary constants. This assumption reduces the mathematical complexity of the system and facilitates the derivation of exact cosmological solutions.

The effective or average scale factor is

$$a = (A^2 B)^{1/3} \tag{20}$$

The Volume scale factor V can be written as

$$V = a^3 = \sqrt{-g} = A^2 B \tag{21}$$

Using equations (18),(19) and(20),we get

$$A(t) = [k_5 (k_3 t + k_4)]^{1/k_5}, \text{where } k_5 = \frac{(k_1 + 2)(k_2 + 3)}{3} \tag{22}$$

where k_3 and k_4 are the integration constants.
From (18) and (22), we have

$$B(t) = [k_5 (k_3 t + k_4)]^{k_1/k_5} \tag{23}$$

Therefore, the corresponding metric can be expressed as

$$ds^2 = dt^2 - [k_5 (k_3 t + k_4)]^{2/k_5} \left[dx^2 + f^2 d\Phi^2\right] - [k_5 (k_3 t + k_4)]^{2k_1/k_5} dz^2 \tag{24}$$

We ascertain the cosmos's scale factor utilising equations (20), (22), and (23) as follows:

$$a(t) = [k_5 (k_3 t + k_4)]^{\frac{2+k_1}{3k_5}} \tag{25}$$

Therefore, from equations (19) and (25), we derive the scalar field as

$$\phi = \phi_0 [k_5 (k_3 t + k_4)]^{\frac{k_2}{k_2+3}} \tag{26}$$

We determine the Hubble's parameter from equation (25) as

$$H = \frac{\dot{a}}{a} = \frac{k_3(2 + k_1)}{3k_5(k_3 t + k_4)} \tag{27}$$

The Deceleration parameter equation is as follows $q = \frac{-\ddot{a}(t)}{a(t) H^2}$
Equations (25) and (27) can be used to calculate the deceleration parameter.

$$q = \frac{3k_5}{2 + k_1} - 1 \tag{28}$$

The Anisotropic parameter is described as

$$A_h = \frac{1}{3} \sum_{i=1}^{3} \left(\frac{H_i - H}{H}\right)^2 = \frac{6\left(k_1^2 + 2k_1 + 3\right)}{(k_1 + 2)^2} \tag{29}$$

The Expansion scalar is defined as $H = \frac{\theta}{3}$ so $\theta = 3H$
Equation (27) can be used to calculate the Expansion scalar as

$$\theta = \frac{k_3(2+k_1)}{k_5(k_3t+k_4)} \tag{30}$$

The redshift z is defined as $z = \frac{a_0}{a} - 1$
Using equation (25), and by considering $a_0 = 1$
Redshift for our model is given by

$$z = \frac{1 - [k_5\,(k_3t+k_4)]^{\frac{2+k_1}{3k_5}}}{[k_5\,(k_3t+k_4)]^{\frac{2+k_1}{3k_5}}} \tag{31}$$

,
Energy Density of Sharma-Mittal Holographic Dark Energy is defined as

$$\rho_{de} = \frac{3k^2H^4}{8\pi s}\left[\left(1+\frac{\pi l}{H^2}\right)^{\frac{s}{l}} - 1\right]$$

where k is a dimensionless constant, s and l are Sharma–Mittal entropy parameters corresponding to deformation and non-extensivity and H is Hubble's parameter.The parameter l measures the deviation from standard extensive thermodynamics, whereas s controls the deformation effect of the generalized entropy structure. An important feature of Sharma–Mittal entropy is that it reduces to Tsallis entropy in the limit $s \to l$, and to Rényi entropy in the limit $s \to 0$. Hence, Sharma–Mittal entropy provides a more general and physically consistent framework for describing gravitational systems with long-range interactions and non-additive thermodynamical behavior.
By substituting H value in the above equation from (27), we get energy density as

$$\rho_{de} = \frac{3k^2}{8\pi s}\left[\frac{k_3\,(2+k_1)}{3k_5}\right]^4\left[\frac{1}{(k_3t+k_4)^4}\right]\left[\left[1+\frac{9k_5^2(k_3t+k_4)^2l\pi}{k_3^2(2+k_1)^2}\right]^{\frac{s}{l}} - 1\right] \tag{32}$$

For plotting the graphical behavior of the cosmological parameters, we have considered the values $k = 0.7$, $k_1 = 2.01$, $k_2 = 1.01$, $k_3 = 0.45$, $k_4 = 3.5$, $s = 4.5$, $l = 6$, $a_0 = 1$, $k_6 = 1.2$ and $\omega = 50$. These chosen values satisfy the physical viability of the model and help in obtaining well-behaved graphical evolution of the cosmological quantities.

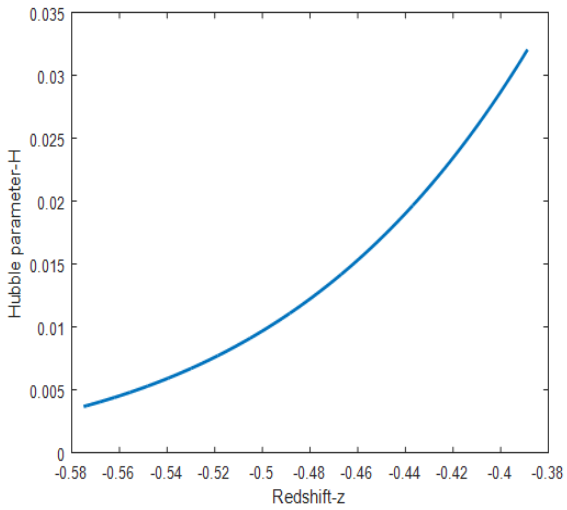

Figure 1. The Hubble parameter against redshift

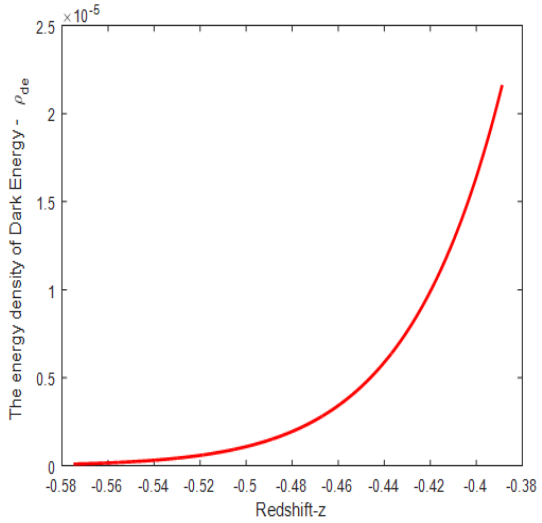

Figure 2. The DE's energy density against redshift

The equation that we will use to acquire the EoS parameter is as follows.

$$\omega_{de} = -1 - \frac{\rho'_{de}}{3H\rho_{de}}$$

Equations (27) and (32) can be used to calculate the EoS parameter of the model as

$$\omega_{de} = -1 + \frac{4k_5}{k_1+2} - \frac{\frac{18s\pi k_5^3[k_3t+k_4)^2}{k_3^2(2+k_1)^3}\left[1+\frac{9k_5^2(k_3t+k_4)^2l\pi}{k_3^2(2+k_1)^2}\right]^{\frac{s}{l}-1}}{\left[1+\frac{9k_5^2(k_3t+k_4)^2l\pi}{k_3^2(2+k_1)^2}\right]^{\frac{s}{l}}-1} \tag{33}$$

We can determine the matter's energy density using equations (12) and (32). Then

$$\rho_m = \frac{3k^2}{8\pi s}\left[\frac{k_3\,(2+k_1)}{3k_5}\right]^4\left[\frac{1}{(k_3t+k_4)^4}\right]\left[\left[1+\frac{9k_5^2(k_3t+k_4)^2l\pi}{k_3^2(2+k_1)^2}\right]^{\frac{s}{l}}-1\right]$$

$$+\frac{k_3^2\phi_0}{8\phi}[k_5\,(k_3t+k_4)]^{\frac{k_2}{k_2+3}-2}\left\{\begin{array}{c} 1+2k_1+(2+k_1)\,k_2k_5 \\ -\frac{k_2^2k_5^2}{2(k_2+3)^2}\left(-1+\frac{4k_5}{k_1+2}-\frac{\frac{18s\pi k_5^3[k_3t+k_4)^2}{k_3^2(2+k_1)^3}\left[1+\frac{9k_5^2(k_3t+k_4)^2l\pi}{k_3^2(2+k_1)^2}\right]^{\frac{s}{l}-1}}{\left[1+\frac{9k_5^2(k_3t+k_4)^2l\pi}{k_3^2(2+k_1)^2}\right]^{\frac{s}{l}}-1}\right) \end{array}\right\} \tag{34}$$

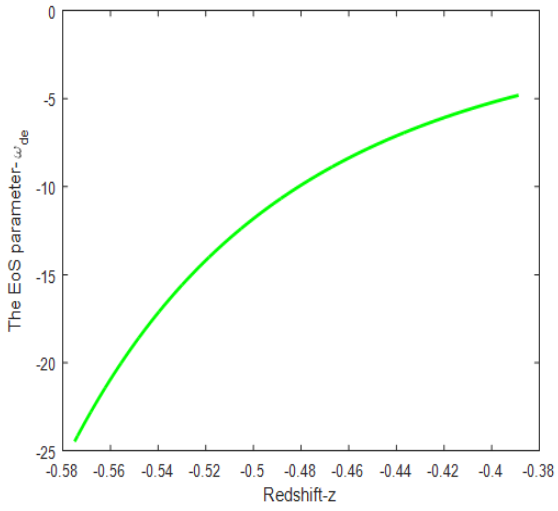

Figure 3. The EoS parameter against redshift

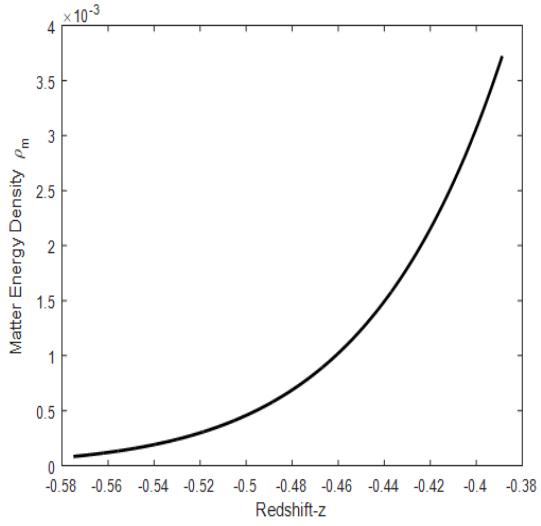

Figure 4. The energy density of matter against redshift

Hence from equations (27) and (33), we find the pressure of DE as

$$p_{de} = -\frac{\phi_0k_3^2[k_5\,(k_3t+k_4)]^{\frac{k_2}{k_2+3}-2}}{16\pi(k_2+3)^2}\left\{k_6+k_2^2k_5^2\left[-1+\frac{4k_5}{k_1+2}-\frac{\frac{18s\pi k_5^3[k_3t+k_4)^2}{k_3^2(2+k_1)^3}\left[1+\frac{9k_5^2(k_3t+k_4)^2l\pi}{k_3^2(2+k_1)^2}\right]^{\frac{s}{l}-1}}{\left[1+\frac{9k_5^2(k_3t+k_4)^2l\pi}{k_3^2(2+k_1)^2}\right]^{\frac{s}{l}}-1}\right]\right\} \tag{35}$$

The jerk parameter is represented by the following formula

$$j = \frac{\dddot{a}}{aH^3}$$

Now, with the use of Equations (25) and (27), we are able to calculate the Jerk Parameter as

$$j = \frac{3\,(k_2+2)\,(2k_2+5)}{k_3\,(k_1+2)} \tag{36}$$

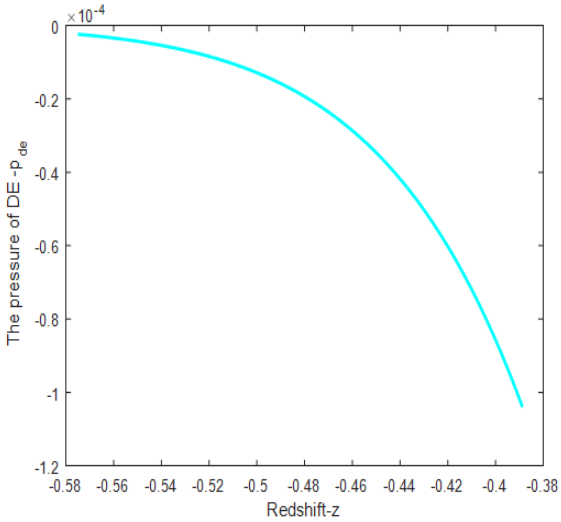

Figure 5. The pressure of DE against redshift

Statefinder Parameters:
The Hubble and deceleration parameters describe the universe's expansion, but because many dark energy models show similar behavior with these, we can't use them to tell the models apart. To fix this, Sahni et.al [30] came up with the statefinder parameters. These act as special cosmological tools to help us better differentiate and understand various dark energy models.These are defined as $r = \frac{\ddot{a}}{aH^3}$ and $s = \frac{r-1}{3(q-\frac{1}{2})}$.
Now, with the use of Equations (25) and (27), we get r as

$$r = \frac{3\,(k_2+2)\,(2k_2+5)}{k_3\,(k_1+2)} \tag{37}$$

and

$$s = \frac{2}{3k_3}\left[\frac{(k_1+2)\,(2k_2+5) - k_3\,(k_1+2)}{k_5 - (2+k_1)}\right] \tag{38}$$

Squared speed of sound: The squared speed of sound, denoted by the symbol v_s^2, is a variable whose sign is used to assess the stability of DE models.The DE model with $v_s^2 > 0$ is considered stable, while the DE model $v_s^2 < 0$ is considered unstable.
From the definition of the sound's squared speed, we have

$$v_s^2 = \frac{\dot{p_{de}}}{\dot{\rho_{de}}}$$

$$v_s^2 = \frac{-\frac{\phi_0 k_3^2 [k_5(k_3t+k_4)]^{\frac{k_2}{k_2+3}-2}}{16\pi(k_2+3)^2}\left\{\frac{-k_3(k_2+6)}{(k_3t+k_4)(k_2+3)}\left[k_6 + k_2^2k_5^2\left[-1+\frac{4k_5}{k_1+2} - \frac{\frac{18s\pi k_5^3[k_3t+k_4)^2}{k_3^2(2+k_1)^3}\left[1+\frac{9k_5^2(k_3t+k_4)^2l\pi}{k_3^2(2+k_1)^2}\right]^{\frac{s}{l}-1}}{\left[1+\frac{9k_5^2(k_3t+k_4)^2l\pi}{k_3^2(2+k_1)^2}\right]^{\frac{s}{l}}-1}\right]\right] + k_2^2k_5^2\left[\frac{\frac{36s\pi k_5^3(k_3t+k_4)^3}{k_3^3(2+k_1)^5}\left[1+\frac{9k_5^2(k_3t+k_4)^2l\pi}{k_3^2(2+k_1)^2}\right]^{\frac{s}{l}-1}}{\left[\left[1+\frac{9k_5^2(k_3t+k_4)^2l\pi}{k_3^2(2+k_1)^2}\right]^{\frac{s}{l}}-1\right]^2}\right.\right.}{\frac{3k^2}{8\pi s}\left(\frac{k_3(2+k_1)}{3k_5}\right)^4\left[\begin{array}{l} -4k_3(k_3t+k_4)^{-5}\left(\left\{1+\frac{9k_5^2(k_3t+k_4)^2l\pi}{k_3^2(2+k_1)^2}\right\}^{\frac{s}{l}}-1\right)+ \\ (k_3t+k_4)^{-4}\frac{s}{l}\left\{1+\frac{9k_5^2(k_3t+k_4)^2l\pi}{k_3^2(2+k_1)^2}\right\}^{\frac{s}{l}-1}\frac{18k_5^2(k_3t+k_4)l\pi}{k_3(2+k_1)^2}\end{array}\right]} \tag{39}$$

$$\left.\left.\left\{\begin{array}{c}\frac{k_3^2(2+k_1)^2}{(k_3t+k_4)^2}+9l\pi\left(\frac{s}{l}-1\right)\left[1+\frac{9k_5^2(k_3t+k_4)^2l\pi}{k_3^2(2+k_1)^2}\right]^{-1} \\ -9k_5^2s\pi\left[1+\frac{9k_5^2(k_3t+k_4)^2l\pi}{k_3^2(2+k_1)^2}\right]^{\frac{s}{l}-1}\end{array}\right\}\right]\right)\right\}$$

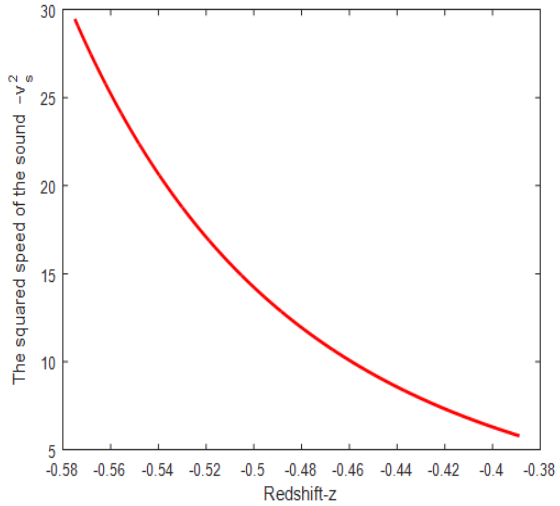

Figure 6. The Squared speed of sound versus redshift

The total density parameter defined as

$$\Omega = \Omega_m + \Omega_{de} \text{ here } \Omega_m = \frac{\rho_m}{3H^2} \text{ and } \Omega_{de} = \frac{\rho_{de}}{3H^2} \tag{40}$$

From equations (27) and (32) we have

$$\Omega_{de} = \frac{k^2}{8\pi s}\left[\frac{k_3\,(2+k_1)}{3k_5}\right]^2\left[\frac{1}{(k_3t+k_4)^2}\right]\left[\left[1+\frac{9k_5^2(k_3t+k_4)^2 l\pi}{k_3^2(2+k_1)^2}\right]^{\frac{s}{l}}-1\right] \tag{41}$$

From equations (27) and (34) we have

$$\begin{aligned}\Omega_m = {} & \frac{k^2}{8\pi s}\left[\frac{k_3\,(2+k_1)}{3k_5}\right]^2\left[\frac{1}{(k_3t+k_4)^2}\right]\left[\left[1+\frac{9k_5^2(k_3t+k_4)^2 l\pi}{k_3^2(2+k_1)^2}\right]^{\frac{s}{l}}-1\right] \\ & + \frac{k_3^2\phi_0}{8\phi}\left[k_5\,(k_3t+k_4)\right]^{\frac{k_2}{k_2+3}-2}\left\{\begin{array}{c} 1+2k_1+(2+k_1)\,k_2k_5 \\ -\frac{k_2^2k_5^2}{2(k_2+3)^2}\left(-1+\frac{4k_5}{k_1+2}-\frac{\frac{18s\pi k_5^3[k_3t+k_4)^2}{k_3^2(2+k_1)^3}\left[1+\frac{9k_5^2(k_3t+k_4)^2l\pi}{k_3^2(2+k_1)^2}\right]^{\frac{s}{l}-1}}{\left[1+\frac{9k_5^2(k_3t+k_4)^2l\pi}{k_3^2(2+k_1)^2}\right]^{\frac{s}{l}}-1}\right)\end{array}\right\}\end{aligned} \tag{42}$$

From equations (40),(41) and (42) we have

$$\begin{aligned}\Omega = {} & \frac{2k^2}{8\pi s}\left[\frac{k_3\,(2+k_1)}{3k_5}\right]^2\left[\frac{1}{(k_3t+k_4)^2}\right]\left[\left[1+\frac{9k_5^2(k_3t+k_4)^2 l\pi}{k_3^2(2+k_1)^2}\right]^{\frac{s}{l}}-1\right] \\ & + \frac{k_3^2\phi_0}{8\phi}\left[k_5\,(k_3t+k_4)\right]^{\frac{k_2}{k_2+3}-2}\left\{\begin{array}{c} 1+2k_1+(2+k_1)\,k_2k_5 \\ -\frac{k_2^2k_5^2}{2(k_2+3)^2}\left(-1+\frac{4k_5}{k_1+2}-\frac{\frac{18s\pi k_5^3[k_3t+k_4)^2}{k_3^2(2+k_1)^3}\left[1+\frac{9k_5^2(k_3t+k_4)^2l\pi}{k_3^2(2+k_1)^2}\right]^{\frac{s}{l}-1}}{\left[1+\frac{9k_5^2(k_3t+k_4)^2l\pi}{k_3^2(2+k_1)^2}\right]^{\frac{s}{l}}-1}\right)\end{array}\right\}\end{aligned} \tag{43}$$

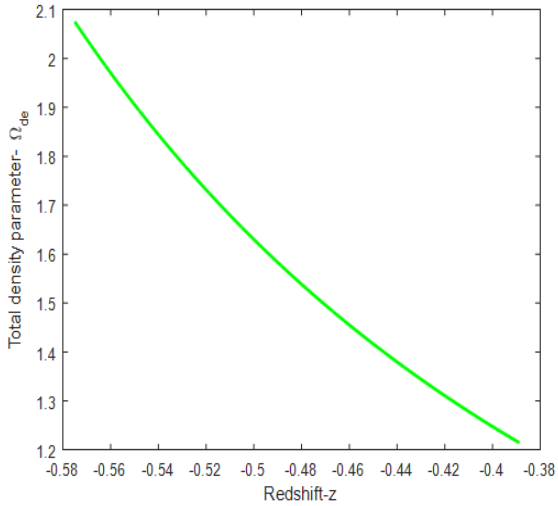

Figure 7. The total density parameter against redshift

The coincidence parameter is defined as

$$\bar{r} = \frac{\rho_{de}}{\rho_m} \tag{44}$$

From equations (32),(34) and (44) we have

$$\bar{r} = \frac{\frac{3k^2}{8\pi s}\left[\frac{k_3(2+k_1)}{3k_5}\right]^4\left[\frac{1}{(k_3t+k_4)^4}\right]\left[\left[1+\frac{9k_5^2(k_3t+k_4)^2l\pi}{k_3^2(2+k_1)^2}\right]^{\frac{s}{l}}-1\right]}{\frac{3k^2}{8\pi s}\left[\frac{k_3(2+k_1)}{3k_5}\right]^4\left[\frac{1}{(k_3t+k_4)^4}\right]\left[\left[1+\frac{9k_5^2(k_3t+k_4)^2l\pi}{k_3^2(2+k_1)^2}\right]^{\frac{s}{l}}-1\right]} + \frac{k_3^2\phi_0}{8\phi}\left[k_5\left(k_3t+k_4\right)\right]^{\frac{k_2}{k_2+3}-2}\left\{\left(-1+\frac{4k_5}{k_1+2}-\frac{\frac{18s\pi k_5^3[k_3t+k_4)^2}{k_3^2(2+k_1)^3}\left[1+\frac{9k_5^2(k_3t+k_4)^2l\pi}{k_3^2(2+k_1)^2}\right]^{\frac{s}{l}-1}}{\left[1+\frac{9k_5^2(k_3t+k_4)^2l\pi}{k_3^2(2+k_1)^2}\right]^{\frac{s}{l}}-1}\right)\right\} \tag{45}$$

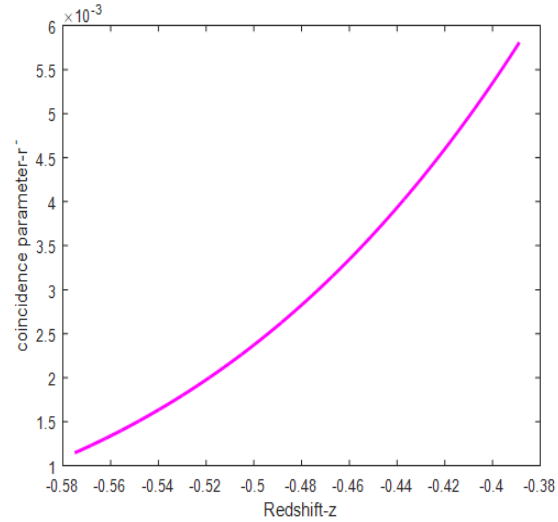

Figure 8. The coincidence parameter against redshift

The $\omega_{de} - \omega'_{de}$ plane: The plane $\omega_{de} - \omega'_{de}$ examination is used to assess the dynamic feature of the DE models evaluated by Steinhardt and Wang [29] where ω'_{de}denotes the derivative in relation to ln a. This approach has utilized the

fundamental model, leading to the creation of two plane models. The interior of the region $(\omega_{de}<0, \omega'_{de}>0)$ is the thawed area, while the area $(\omega_{de}<0, \omega'_{de}<0)$ beneath it is frozen.
The expression for ω'_{de} the derivative of equation (33) w.r.t ln a is obtained as

$$\omega'_{de} = \frac{\frac{36s\pi k_5^3(k_3t+k_4)^3}{k_3^3(2+k_1)^5}\left[1+\frac{9k_5^2(k_3t+k_4)^2l\pi}{k_3^2(2+k_1)^2}\right]^{\frac{s}{l}-1}}{\left[\left[1+\frac{9k_5^2(k_3t+k_4)^2l\pi}{k_3^2(2+k_1)^2}\right]^{\frac{s}{l}}-1\right]^2}\left\{\begin{array}{c}\frac{k_3^2(2+k_1)^2}{(k_3t+k_4)^2}+9l\pi\left(\frac{s}{l}-1\right)\left[1+\frac{9k_5^2(k_3t+k_4)^2l\pi}{k_3^2(2+k_1)^2}\right]^{-1} \\ -9k_5^2s\pi\left[1+\frac{9k_5^2(k_3t+k_4)^2l\pi}{k_3^2(2+k_1)^2}\right]^{\frac{s}{l}-1}\end{array}\right\} \tag{46}$$

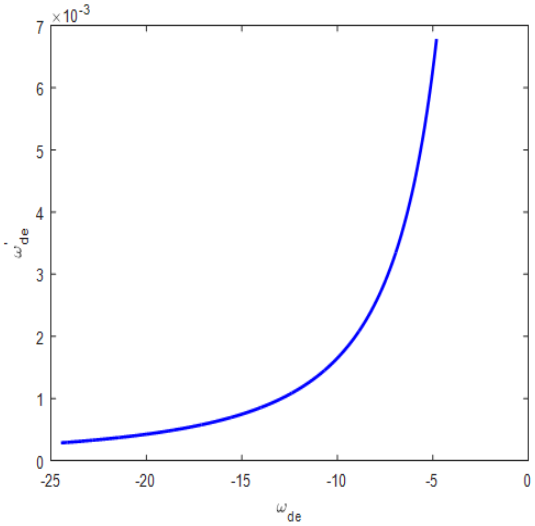

Figure 9. The $\omega_{de} - \omega'_{de}$ plane

4. CONCLUSIONS

In this study, we have investigated an Axially Symmetric Cosmological model within the context of Brans–Dicke theory, incorporating the SMHDE. The modified field equations were derived and analysed to examine the dynamical behaviour of the universe under the combined effects of anisotropy, scalar–tensor coupling, and generalized entropy. Our results demonstrate that the inclusion of Sharma–Mittal entropy significantly alters the evolution of holographic dark energy density, leading to notable modifications in key cosmological parameters. The model successfully describes late-time cosmic acceleration and highlights the crucial role of entropy generalization in shaping the expansion dynamics.

We have taken $k = 0.7$, $k_1 = 2.01$, $k_2 = 1.01$, $k_3 = 0.45$, $k_4 = 3.5$, $s = 4.5$, $l = 6$, $a_0 = 1$, $k_6 = 1.2$ and $\omega = 50$ values to plot the graphs.

- Figure 1 illustrates the relationship between redshift (z) and the Hubble parameter (H). From figure we observe that the Hubble parameter remains positive and decreases. However, the overall trend suggests that the cosmic expansion slows down over time, likely due to gravitational effects or other attractive forces. If this behaviour continues indefinitely, it may indicate a universe that could eventually stop expanding or transition into a slower, steady state of expansion.

- Figure 2 illustrates the relationship between the DE's energy density and redshift (z). The graph shows that the energy density remains positive and decreases. The positive value of the DE's energy density indicates its significant contribution to the total energy content of the cosmos. Moreover, as the redshift increases, the energy density gradually diminishes, suggesting that the cosmos is expanding and that the DE's density decreases progressively over cosmic time.

- Figure 3 illustrates the relationship between the EoS parameter (ω_{de}) and redshift (z). The graph shows that ω_{de} remains negative throughout its evolution and satisfies $\omega_{de} < -1$, indicating a phantom energy regime. Additionally, the EoS parameter decreases as redshift evolves. Since $\omega_{de} < -1$, the cosmos is undergoing accelerated expansion driven by phantom energy dominance. Although the acceleration persists, its magnitude may gradually decrease over cosmic time, depending on the dynamical behavior of the model.

- Figure 4 illustrates the relationship between the DM's energy density (ρ_m) and redshift (z). The graph shows that the dark matter energy density remains positive throughout its evolution and decreases. This behavior is consistent with an expanding universe

- Figure 5, the graph depicts the relationship between the pressure ($\bar{p}_{de}$) of DE and redshift (z). The graph shows that the pressure remains negative throughout its evolution and increases. This negative pressure of SMHDE indicates the presence of a repulsive component responsible for driving cosmic acceleration. As the pressure becomes more negative, the repulsive effect strengthens, thereby enhancing the accelerated expansion of the cosmos. This behavior is consistent with dark energy models that predict an increasing dominance of negative pressure in the cosmic dynamics.

- Figure 6 illustrates the relationship between the squared speed of sound (v_s^2) and redshift (z). The graph shows that v_s^2 remains positive throughout its evolution. The positivity of the squared speed of sound indicates that the model is free from classical instabilities under small perturbations. Therefore, this behavior suggests that the proposed cosmological model is stable over the considered redshift range.

- Figure 7 illustrates the relationship between the total density parameter against redshift.The graph shows that the total density parameter remains positive throughout its evolution and increases.The total density parameter change with redshift is depicted on the graph. Throughout, the overall density value stays positive, suggesting a cosmos with physical significance. Its upward trend indicates that, in comparison to the critical density, the total energy density increases. This demonstrates how the cosmos is entering a period of faster expansion driven by DE.

- Figure 8 illustrates the relationship between the coincidence parameter against redshift.The graph shows that the coincidence parameter remains positive throughout its evolution and decreases**.** Its decreasing behavior with time suggests that the universe evolves from an earlier matter-dominated phase to a late-time dark energy-dominated phase.

- Figure 9, the progression of our model is shown on the $\omega_{de} - \omega'_{de}$ plane. We observe that, depending on the graph values, $\omega_{de} - \omega'_{de}$ the plane trajectories change $\left(\omega_{de}<0, \omega'_{de}>0\right)$ in the thawed region.

Declarations:
Funding: No funds, grants, or other support was received.
Conflicts of interest: The authors have no conflicts of interest to declare that are relevant to the content of this article.
Availability of data and material: The data supporting the findings of this investigation are accessible from the corresponding author upon reasonable request.

Acknowledgements
we are thankful to the respected reviewer for his helpful comments, which have substantially improved the caliber of study and the presentation of our work.

ORCID

Suresh Kadali, https://orcid.org/0009-0004-9221-4483; **Neelima Davuluri**, https://orcid.org/0000-0003-1625-5596

REFERENCES

[1] A. G. Riess, *et al*., "Observational evidence from supernovae for an accelerating universe and a cosmological constant", Astronomical Journal, **116**, 1009 (1998). https://doi.org/10.1086/300499

[2] S. Perlmutter, *et al*., "Measurements of Omega and Lambda from 42 high-redshift supernovae", Astrophysical Journal, **517**, 565 (1999). https://doi.org/10.1086/307221

[3] D. N. Spergel, *et al*., "First-year WMAP observations: determination of cosmological parameters", Astrophysical Journal Supplement Series, **148**, 175 (2003). https://doi.org/10.1086/377226

[4] M. Tegmark, Y. Wang, and M. Zaldarriaga, "New dark energy constraints from supernovae, microwave background, and galaxy clustering", Physical Review Letters, **92**, 241302 (2004). https://doi.org/10.1103/PhysRevLett.92.241302

[5] Carroll, S. M., "The cosmological constant", Living Reviews in Relativity 4, 1 (2001). https://doi.org/10.12942/lrr-2001-1

[6] S. R. Choudhury, *et al*., "Dark energy density from observational constraints", Physics Letters B, **650**, 1–6 (2007). https://doi.org/10.1016/j.physletb.2007.04.010

[7] G. 't Hooft, "Dimensional reduction in quantum gravity," gr-qc/9310026 (1993). https://arXiv:gr-qc/9310026

[8] L. Susskind, "The world as a hologram", Journal of Mathematical Physics, **36**, 6377 (1995). https://doi.org/10.1063/1.531249

[9] A. G. Cohen, D. B. Kaplan, and A. E. Nelson, "Effective field theory, black holes, and the cosmological constant", Physical Review Letters, **82**, 4971 (1999). https://doi.org/10.1103/PhysRevLett.82.4971

[10] M. Li, "A model of holographic dark energy", Physics Letters B, **603**, 1 (2004). https://doi.org/10.1016/j.physletb.2004.10.014

[11] C. Tsallis, "Possible generalization of Boltzmann–Gibbs statistics", Journal of Statistical Physics, **52**, 479 (1988). https://doi.org/10.1007/BF01016429

[12] A. Rényi, *Probability Theory*, (North-Holland Publishing, Amsterdam, 1970). https://www.elsevier.com/books/probability-theory/renyi/978-0-444-10168-1

[13] B. D. Sharma, and D. P. Mittal, "New nonadditive measures of entropy for discrete probability distributions," Journal of Mathematical Sciences, **10**, 28 (1975). https://doi.org/10.1007/BF02303867

[14] A. Jawad, S. Rani, and A. Chaudhry, "Sharma–Mittal holographic dark energy in modified gravity", European Physical Journal C, **77**, 349 (2017). https://doi.org/10.1140/epjc/s10052-017-4914-2

[15] A. Iqbal, and A. Jawad, "Cosmological behaviour of Sharma–Mittal holographic dark energy models", European Physical Journal C, **79**, 982 (2019). https://doi.org/10.1140/epjc/s10052-019-7497-9

[16] S. Maity, and U. Debnath, "Dynamics of Sharma–Mittal holographic dark energy models", Modern Physics Letters A, **34**, 1950356 (2019). https://doi.org/10.1142/S0217732319503563

[17] S.H. Shekh, and U. Debnath, "Stability of Sharma–Mittal holographic dark energy in anisotropic cosmology", International Journal of Geometric Methods in Modern Physics, **18**, 2150027 (2021). https://doi.org/10.1142/S0219887821500274

[18] C. Brans, and R. H. Dicke, "Mach's principle and a relativistic theory of gravitation", Physical Review, **124**, 925 (1961). https://doi.org/10.1103/PhysRev.124.925

[19] O. Bertolami, and P. J. Martins, "Nonminimal coupling and quintessence", Physical Review D, **61**, 064007 (2000). https://doi.org/10.1103/PhysRevD.61.064007

[20] V. Faraoni, *Cosmology in Scalar-Tensor Gravity*", (Kluwer Academic Publishers, Dordrecht, 2004). https://link.springer.com/book/10.1007/978-1-4020-1989-2

[21] M. R. Setare, and M. Jamil, "Holographic dark energy in non-flat Brans-Dicke cosmology", Journal of Cosmology and Astroparticle Physics, **03**, 010 (2010). https://doi.org/10.1088/1475-7516/2010/03/010

[22] S. Ghaffari, H. Hossienkhani, and T. Azizi, "Interacting holographic dark energy in Brans-Dicke theory", Astrophysics and Space Science, **361**, 161 (2018). https://doi.org/10.1007/s10509-016-2734-0

[23] B. Kiran, and D. R. K. Reddy, "Minimally interacting HDE models in Brans-Dicke theory", Modern Physics Letters A, **36**, 2150011 (2021). https://doi.org/10.1142/S0217732321500110

[24] V. U. M. Rao, and K. V. S. Sireesha, "Axially symmetric perfect fluid cosmological models in Brans-Dicke theory", African Review of Physics, **7**, 54 (2012). http://lamp3.tugraz.at/ hadley/arp/arp.html

[25] B. Saha, and P. Mondal, "Anisotropic dark energy cosmology in Brans-Dicke gravity", European Physical Journal C, **82**, 567 (2022). https://doi.org/10.1140/epjc/s10052-022-10494-2

[26] V. B. Johri, and R. Sudharshan, "Power-law Expansion and Inflation in Brans–Dicke Theory", Australian Journal of Physics, **42**(2), 215–222 (1989).

[27] V. B. Johri and K. Desikan, "Cosmological Models with Constant Deceleration Parameter in Brans–Dicke Theory," General Relativity and Gravitation, **26**, 1217–1232 (1994). https://doi.org/10.1007/BF02106714

[28] D. Trivedi and A.K. Bhabor, "Higher Dimensional Bianchi Type-III String Cosmological Models with Dark Energy in Brans–Dicke Scalar-Tensor Theory of Gravitation," New Astronomy, **89**, 101658 (2021).https://doi.org/10.1016/j.newast.2021.101658

[29] R. R. Caldwell, and E. V. Linder, "The Limits of Quintessence", Physical Review Letters, **95**, 141301 (2005). https://doi.org/10.1103/PhysRevLett.95.141301

[30] V. Sahni, T. D. Saini, A. A. Starobinsky, and U. Alam, "Statefinder A New Geometrical Diagnostic of Dark Energy," Journal of Experimental and Theoretical Physics Letters (JETP Letters), **77**(5), 201–206 (2003). https://doi.org/10.1134/1.1574831

АКСІАЛЬНО СИМЕТРИЧНА ГОЛОГРАФІЧНА ТЕМНА ЕНЕРГІЯ ШАРМА-МІТТАЛА В ТЕОРІЇ БРАНСА-ДІККЕ

Суреш Кадалі, **Ніліма Давулурі**

Кафедра математики та статистики, GITAM, (вважається університетом), Вішакхапатнам-530045, Індія

Це дослідження вивчає голографічну темну енергію Шарма-Міттала (SMHDE) в контексті теорії гравітації Бранса-Дікке в аксіально симетричній космологічній моделі. Використовуючи ентропію Шарма-Міттала, яка забезпечує об'єднуюче узагальнення ентропій Цалліса та Реньї, формулюється модифікована форма густини голографічної темної енергії для врахування неекстенсивних термодинамічних ефектів. Відповідні рівняння поля виведені та розв'язані для отримання точних аналітичних рішень. Крім того, ключові космологічні параметри, такі як параметр EoS, параметр уповільнення та квадрат швидкості звуку, систематично аналізуються для вивчення динамічної поведінки та стабільності моделі. Результати показують, що запропонована структура успішно описує прискорене розширення космосу наприкінці часу, а також враховує можливі анізотропії в ранньому космосі. Загалом, модель являє собою послідовне та фізично життєздатне розширення традиційних голографічних сценаріїв темної енергії в рамках скалярно-тензорної гравітаційної теорії.

Ключові слова: *ентропія Шарми-Міттала; голографічна темна енергія; Теорія Бранса-Дікке; аксіально-симетрична метрика*